Paweł BALUKA[1]
Marian KUZMA[1,2]

OPTICAL FEEDBACK.
II DYNAMIC EFFECTS

Abstract: In the present paper the mathematical model, introduced by Crutchfield [1], for video feedback performance is outlined. The two dynamical fractals observed in our video feedback experiment have been described. The first one shows the five-fold symmetry. Its spatial form relates well to the one which was simulated numerically by Andersen [2]. The second one consists of black strips with dislocations and rotates with the velocity of 0.2 $1/s^{-1}$. The spatial form looks like a modern picture and its spatial time evolution correlates well with Chopin music.

Keywords: video feedback, fractals, time evolution, attractors.

1. INTRODUCTION

Space-time behaviour of dynamic systems is very complex. This behaviour is described by the solution of differential equation, or equivalently, by iteration. There are numerous dynamic systems in physics, technics, electronics, biology, sociology, medicine, and the like. The system consisting of a monitor, a computer and a camera is very easy to set up, and enables to observe the rich of space-time feedback solutions of the system in question. Even a small change of control parameters causes some drastic changes of the pictures which demonstrate solutions. The experiment and its results were described in many papers and books, see for example [3,4]. In the first part of our work [5] (called Paper I), the experiment was described and the static (equilibrium) results were presented for particular control parameters. In the present paper, the mathematical models of the optical feedback introduced by J.M. Crutchfield [1] are addressed in Section 2. In accordance with that paper, we have divided the dynamic effects of the optical feedback into categories (Section 3). In the experimental part (Section 4), some complex video results will be presented. The dynamic space-time image representing the dislocation category will be presented in the form of a video.

---

[1]   Technical College, State Academy of Applied Science in Przemyśl, Książąt Lubomirskich 6, 37-700 Przemyśl, Poland

[2]   Correspondence: Marian Kuzma, Technical College, State Academy of Applied Science in Przemyśl, Książąt Lubomirskich 6, 37-700 Przemyśl, Poland; tel. 500 456 246, mkuzma@ur.edu.pl; Institute of Material Engineering, College of Natural Sciences, University of Rzeszow, Rzeszow, Rejtana Str 16a. 35-959 Rzeszow, Poland

2. MATHEMATICAL MODEL

Mathematical descriptions of the optical feedback are based on mathematical theory of dynamic systems. One of the first such descriptions is the Crunchfield model [1]. This model is an adoption of the idea of a mathematical description of the morphogenesis phenomenon. This model, created by Turing in 1952 [6], is widely used in chemistry and biology, and is known as reaction-diffusion (RD). It adequately explains the phenomena of the self-regulated patterns in biological materials. In his work, Turing studied embryo morphogenesis based on temporal evolution of a cells system with two substances (morphogens), chemically reacting with each other, diffusing between cells, and having a concentration gradient of these substances. The model can be adopted to other systems with more morphogens, which may not necessarily be concentrations. It can also be applied to a continuous system in space. The general form of the model is :

$$d\mathbf{f}/dt = F(\mathbf{f}) + D \nabla^2 \mathbf{f} \tag{1}$$

where $\mathbf{f}$ is the field $\mathbf{f} = (\mathbf{f}_1, \mathbf{f}_2...\mathbf{f}_N)$, D is the diffusion coefficient , ∇^2 is the Laplace operator.

The first term on the right is a 'reaction' term, and the second one is a 'diffusion' term. In this formalism the state of the system is described as a point in a state space *F,* also called a configuration space. The dynamic of the system is the transformation T of the space relative to oneself in each raster time, T: $F \rightarrow F$. This transformation can be expressed by iteration, or by differential equation. In the video feedback the started state is a picture on the monitor, and it is a collection of values: $I_o(\mathbf{x})$, where $I_o(\mathbf{x})$ is the intensity at the point $\mathbf{x}$ on the screen The $I(\mathbf{x})$ takes values in the range [-1,1]. For $I(\mathbf{x})$ = -1 the point $\mathbf{x}$ is in black colour and for $I(\mathbf{x})$ = 1 the point is in white colour. After time equal to n raster times, the intensity at point $\mathbf{x}$ is $I_n(\mathbf{x})$. Thus, the transformation T can be expressed as discrete-time transformation of spatially continuous function I_n, into the set of function I_{n+1} :

$$T : I_n(\mathbf{x}) \rightarrow I_{n+1}(\mathbf{x}) \quad \text{for } \mathbf{x} \in \underline{R}^2 \tag{2}$$

Vector $\mathbf{x} = (x_1, y_1)$ is the point from a bounded plane $\underline{\mathbf{R}}^2$ representing the screen (Fig.1a):

$$\underline{\mathbf{R}}^2 = [-1, 1] \times [-1, 1] \tag{3}$$

In a model for colour feedback, the intensity I ($\mathbf{x}$) is treated as a vector $\mathbf{I}(\mathbf{x})$ with three components corresponding to red R($\mathbf{x}$), green G($\mathbf{x}$), and blue B($\mathbf{x}$) intensities:

$$\mathbf{I}(x) = (R(x), G(x), B(x)) \tag{4}$$
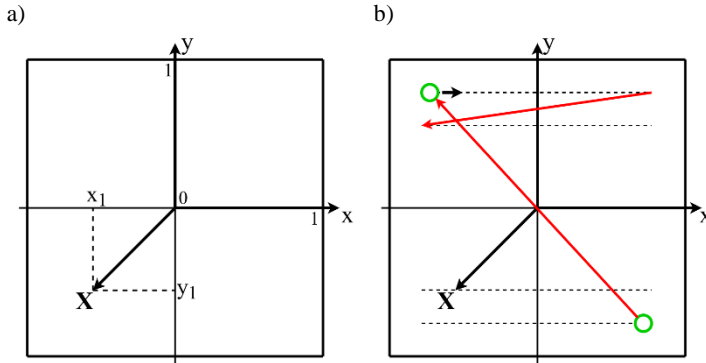
a)   b)

Fig. 1. Screen as a bounded plane; continuous
– space plane (a), discrete – space plane (b).

In the first optical feedback experiments (4), the apparatus consisted only of a CRT (cathode-ray tube) monitor and a vidicon camera tube. Both of these devices used electron beams that scanned a matrix with a photosensitive semiconductor layer (camera), or a phosphor-coated screen (monitor). The combination of the monitor and the camera had to take into account horizontal and vertical synchronization. Horizontal scanning was continuous, while vertical scanning was discrete (Fig. 1b). Today, LCD monitors and CCD cameras are appropriate. Both devices are based on matrices. In an LCD monitor, the matrix is created by pixels formed from liquid crystals, in which molecules are controlled by a transistor. In a CCD camera, the matrix is also formed by pixels which are photodiodes or MOS capacitors. The recorded image is discrete both horizontally and vertically (Fig.1b). The resolution, that is, the number of pixels in both the monitor and the camera, is so high that both images can be treated as quasi-continuous. In the time space both technologies (old and new ones) use raster image transmission, thus both an iterative description of the phenomenon and that using a differential equation can be appropriate.

Both models 'iterated' and 'differential equation' make an assumption that at the time t there are both an old image and a new, incoming one, on the screen or in the camera.

J.P. Crutchfield [1] adopted the reaction-diffusion model to video feedback and expressed the equation (1) as:

$$\frac{d\mathbf{I(x)}}{dt} = L\mathbf{I(x)} + sf\mathbf{I}(bR\mathbf{x}) + \sigma\nabla^2\mathbf{I(x)} \tag{5}$$

where the first term on the right is the old image, the second term is an incoming image, and third one is the diffusion coupling term with the diffusion rate described by the matrix σ, and ∇^2 being the Laplace operator.

The parameters in equation (5) are:
- **L** is the matrix of the intensity dissipation of monitor pixels (phosphor grains), and photoconductor chips in the camera,
- b is a magnification of the camera or a magnification executed by a camera-monitor distance,
- R is a rotation matrix; φ is a monitor–camera angle:

$$R = \begin{pmatrix} \cos(\phi) & \sin(\phi) \\ -\sin(\phi) & \cos(\phi) \end{pmatrix} \tag{6}$$

- f is the intensity scaling parameter $f \in [0,1]$, which can describe the degree of darkness in the laboratory or the intensity of ambient light.
- s is equal to -1, or 1 depending on the luminance inversion.

It is not possible to find the exact solution of the equation (5), therefore, numerical methods are used converting equation (5) to an iterated functional equation:

$$\mathbf{I_{n+1}(x)} = \bar{L}\langle\mathbf{I_n(x)}\rangle_t + \bar{L}'\langle\mathbf{I_n(x)}\rangle_x + sf\mathbf{I_n}(bR\mathbf{x}) \tag{7}$$

where $\bar{L}$ and $\bar{L}'$ are matrices which control colour intensity decay and the coupling of the colour signals in the present and incoming images, respectively.

For black-white video feedback the problem is considerably simpler, as the vector $\mathbf{I_n(x)}$ is now a scalar $I_n(\mathbf{x})$. Therefore:

$$I_{n+1}(\mathbf{x}) = LI_n(\mathbf{x}) + L'\langle I_n(\mathbf{x})\rangle_x + sfI_n(bR\mathbf{x}) \tag{8}$$

3. DYNAMIC FORMS OF VIDEO-FEEDBACK

The solutions of equation (7) or (8) depend on parameters s, f, b, L and may have a very complicated space-time dynamic form containing attractors, bifurcations points, and other singularities. Many of these solutions are fractals [4].

Crutchfield [1] proposes the following categories of video feedback images and their attractors (see Table II in [1]):
1. Equilibrium image - attractor: fixed point,
2. Temporally repeating images - attractor: limit cycle,
3. Temporally aperiodic images - attractor: chaotic attractor,
4. Random relaxation oscillation - attractor: limit cycle with noise-modulated stability,
5. Spatially decorrelated dynamics e.g. dislocation - attractor: quasi-attractor,

6. Spatially complex images - attractor: spatial attractor like fixed point, limit cycle,
7. Spatially and temporally aperiodic-attractor: nontrivial combination of the base attractors (point, cycle, chaotic).

Category 1 was described in Paper I and it collects static images for a particular set of parameters.

We have compared categories 2,3 with the solutions of the feedback controller used widely in electro-technique and electronics (e.g. PID controller [8]). The scheme of such feedback and its reaction on external perturbation is presented in Fig. 2.
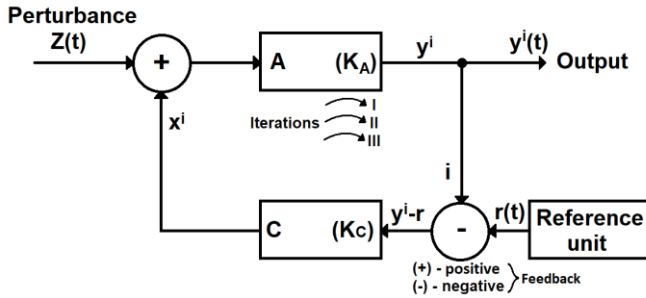

Fig. 2. Scheme of a closed-loop controller (feedback controller
with a perturbation signal and a reference unit)

The system presented in Fig 2. consists of unit A (with the magnification factor K_A), which is controlled by unit C (controller) having the magnification factor K_C. The input signal x(t) is a sum of the iterated signal x^i, and perturbation z(t). Controller C takes the difference between reference r(t), and output y(t) to change the input to system A. The reference input can be set up to a desired constant value $r(t) = r_o$, called 'the set point'.

Then, the initial output from the regulator C is:

$$x = K_C (r_o - y) \tag{9}$$

At the first iteration this input is summed with perturbance z:

$$x^I = K_C (r_o - y) + z \tag{10}$$

The output is then

$$y^I = K_A K_C r_o - K_A K_C y + K_A z . \tag{11}$$

If the system is matched up properly, it means that $y^I \approx y$ than,

$$y = (K_A \ K_C r_o) / (1+K_A K_C) +(K_A z) / (1+ K_A K_C). \qquad (12)$$

Depending on the product $K_A K_C$, there are three types of performance of the system:

1. Stable (for $K_A \ K_C < 1$) (see Fig. 3b and Fig. 3c),
2. With oscillation (for $K_A \ K_C = 1$) (see Fig. 3d),
3. Nonstable (for $K_A \ K_C > 1$) (see Fig. 3e).

The overall magnification factor $K_A K_C$ relates to the monitor-camera distance L in the video feedback system presented in Fig.10 in Paper I. The distance $L = L_o$ results in the magnification $K_A K_C = 1$, for $L < L_o$ the $K_A K_C > 1$, whereas for $L > L_o$ the $K_A K_C < 1$.
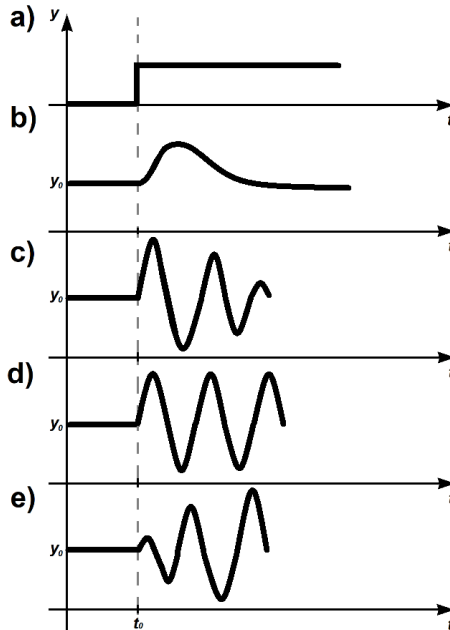
Fig. 3. Types of response of the feedback with reference signal on a step
perturbation: perturbation (a), stable (b, c): oscillating (d); non-stable (e)

4. EXPERIMENTAL PART

4.1. Video feedback set-up

Experiments with video feedback can be performed with a set-up assembled even at home, as it only requires a video camera and a TV or computer monitor or computer. We have described the set-up in details in Paper I. Its general overview is presented in Fig. 4.

The following devices have been used in this experiment:
Computer: NTT BUSINESS W914G
B. Internet camera CREATIVE, type: VFD640,
C. Monitor NEC, type: AS221M;
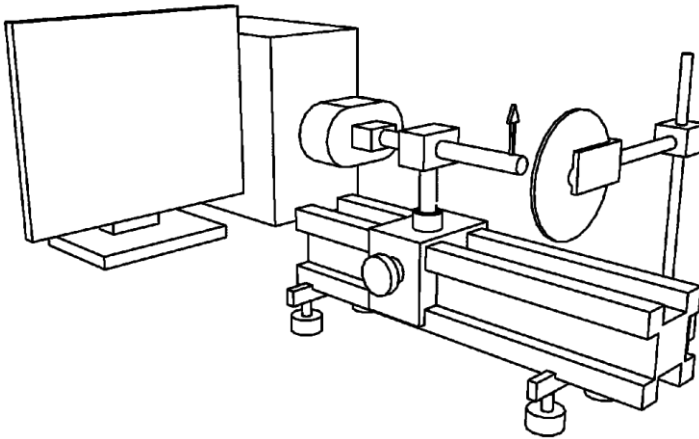
Fig. 4. Video-feedback set-up

4.2. Video feedback parameters

In Table 1 feedback parameters which control the experiments have been collected. These were divided into those connected with a monitor, a camera and the inter-relation monitor-camera.

Table 1. Parameters of video feedback

Monitor		Camera		Monitor-Camera	
Parameter	Value	Parameter	Value	Parameter	Value
Resolution	1680x1050pixel	Resolution	640x480pixel	Distance L	51-64cm
Contrast	50% (middle)	Shutter	auto	Angle α	0°-360°
Brightness	middle	Focus	auto	Zoom at L=55cm	0.94
		Zoom	nominal	Zoom at L=61cm	0.98

5. RESULTS AND DISCUSSION

5.1. Video feedback dynamics for parameters L = 55cm, α = 70 (+-2)

The experimental result for parameters L = 55 cm, α = 70° is a dynamic picture which is evaluated in time (see the video recorded [13]). The magnification for these parameters is M = 0.94. The characteristic patterns recorded at different time t are demonstrated in Fig. 5.

The initial pattern presented in Fig. 5a is a regular five-polygon. After the time t=1s, a bright polygon appears inside (Fig. 5b). Its size decreases with time. Moreover, a five-ray star appears behind the polygon (Fig. 5c). The structure of the rays consists of easily noticeable spots. The shape and the position of the star is stable with time. The origin of the five-fold symmetry of the pattern is the angle α =70°, while 360/ 70 ≈ 5.
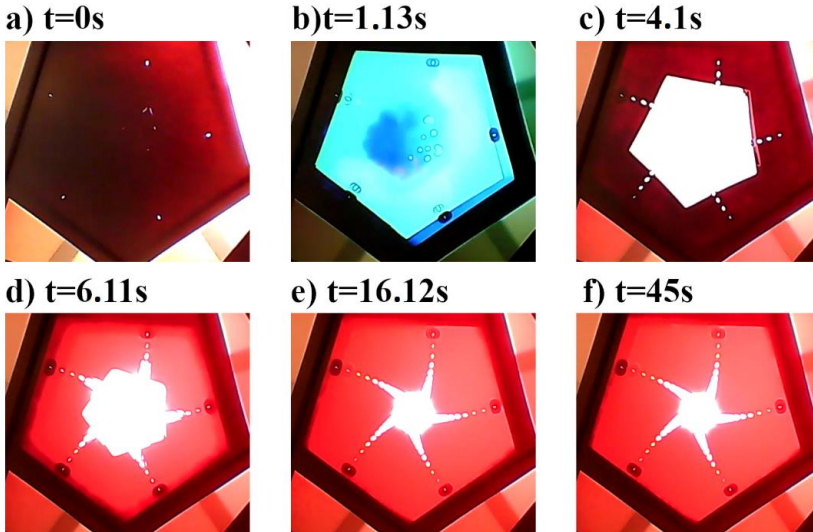
Fig. 5. Samples of dynamical fractal (L = 55, α = 70°), video [13]

After sufficiently long time (t ≈ 16s), the shape of the pattern does not change (see Figs. 5e,f). This final pattern is an attractor. The dynamic of the presented in Fig.5 pattern is not complex and is stabilised into attractor in a relatively short time. This simplicity allows to understand the action of the feedback system. The spots forming rays in Fig. 6 are numbered according to each iteration. It means that a particular iteration results in jumping of a spot from a ray into the next one. Thus, the enumeration of the spots in a ray is modulo 5, e.g. 1,6,11, etc.

The set of five spots from different rays forms an orbit. There are four orbits in Fig. 6:

$$\{1,2,3,4,5\}, \{6,7,8,9,10\}, \{11,12,13,14,15\}, \{16,17,18,19,20\}. \qquad (13)$$

The size of spots increases and their shape resembles an ellipse. The distance from the origin of the picture is changed as well. The size of spots 2D as an average value of a long D_1, and a short D_2 diameters of the ellipse have been measured. The measurements are made in pixels and are collected for twenty spots in Table 2. The distance r of spots from the origin of the pattern is measured in pixels as well. The error of measurements is $\Delta \pm 5$ pixels, when the resolution is not high. Table 2 shows the time t[s], in which the next iterated spot appears. It was calculated from the recorded video [13].
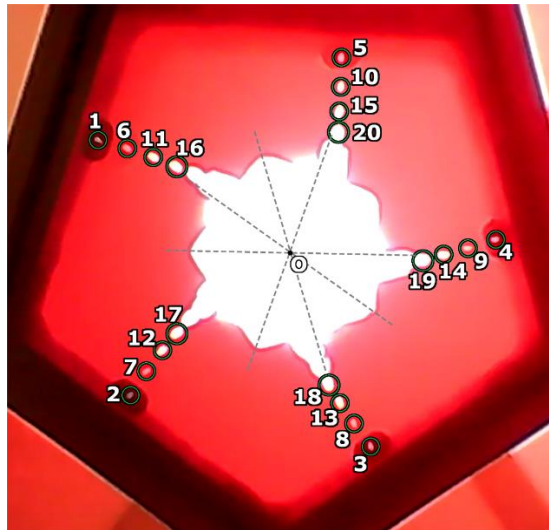
Fig. 6. Dynamic image for L= 55cm, α=70º (±2º), t=7.02s

It is easy to notice in this record that each iteration appears every two frames. The video record was made in the frame of 24 fps (fps – frame per sec.). Owing to this data, it is easy to conclude that every iteration needs time 2/24 [s] = 0.083 s. In Table 2 the averaged diameters of spots for particular orbits are presented. There is also an averaged time of generation of the next orbit.

In Fig. 7. the results of measurements in form of diagrams are presented. The diagrams in Fig.7a and 7b clearly demonstrate the orbital evolution of the shape and radial position of the spots. The effect of increasing the size of spots at every

iteration reflects well spatial diffusion which produces spatial coupling to neighbouring pixels [1]. This effect is described by the third term on the right of equations (7) and (8).

Table 2. Size of spots in form of an ellipse (see Fig. 6): D_1, D_2 are long and short axis respectively, D_{av} is an averaged value of both axes, r is the distance of a spot from the origin of the pattern. Time t is the time at which the spot appears.

Spot No.	Time	D_1	D_2	D_{av}	r
	[s]	[pixel]			
1.	0.083	12.2	5	14.7	348.3
2.	0.167	12	8.5	16.25	328.7
3.	0.250	13	8.5	17.25	310.7
4.	0.333	12.6	7.2	16.2	304.1
5.	0.417	13	10	18	309.8
6.	0.500	13.9	9.4	18.6	305.4
7.	0.583	14.1	6.4	17.3	287.4
8.	0.667	12.2	7.2	15.8	269.8
9.	0.750	13.3	8.1	17.35	261.3
10.	0.833	16.1	11.2	21.7	266.8
11.	0.917	18.9	11.4	24.6	263.8
12.	1.000	17	11.4	22.7	248.9
13.	1.083	16.6	10.8	22	232.8
14.	1.167	19.1	13.2	25.7	224
15.	1.250	20.1	15	27.6	230
16.	1.333	23.7	13.6	30.5	228
17.	1.417	28.3	20.8	38.7	215.5
18.	1.500	25.5	17	34	199.1
19.	1.583	25.2	19.2	34.8	193.1
20.	1.667	27.7	22.4	38.9	195.4
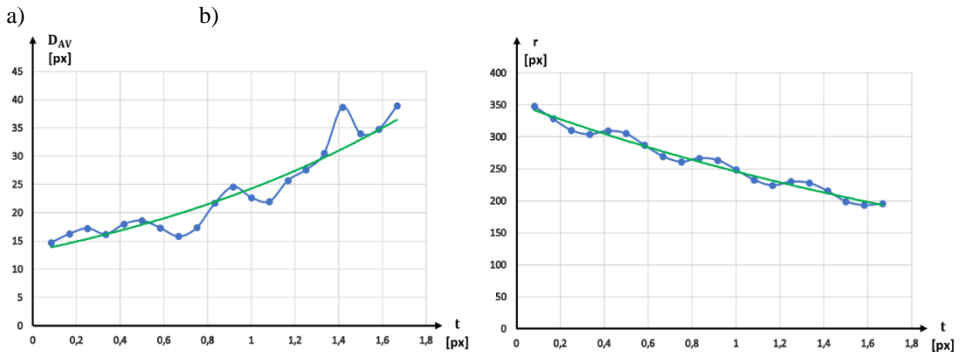
Fig. 7. Size of spots (a), and their radial position (b)

Table 3. Averaged diameters of spots in orbits

Orbit	Spots No.	D_{av} [px]	r_{av} [px]	t_{av} [s]
1	1,2, 3,4,5	12.56	320.32	0.083
2	6,7,8,9,10	13.92	278.14	0.417
3	11,12,13,14,15	18.34	239.9	0.833
4	16, 17, 18 19, 20	26.08	206.22	1.25

5.2. Video feedback dynamics for parameters L = 59cm, α = 85° (±2°)

The second case of video feedback is shown in Fig. 8. In this figure the samples of a dynamic fractal generated by video feedback at control parameters L = 59 cm, α = 85°(±2°) are presented. The rich and interesting time evolution of this fractal is recorded at web site [14].
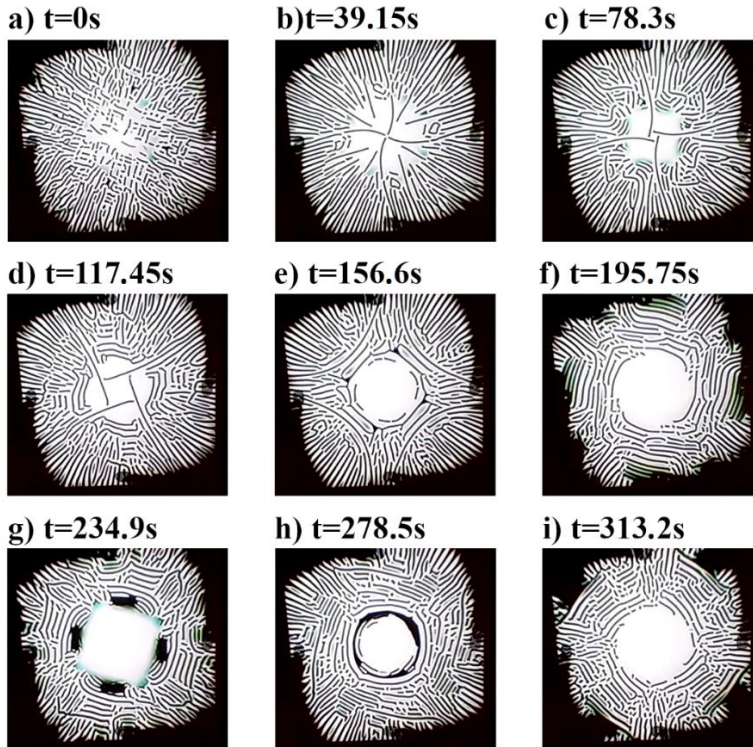
Fig. 8. Time samples for video feedback: L = 59cm, α = 85° (±2°)

The overall pattern consists of dark strips which rotate with the velocity of 0.2 1/s. We have noticed that the evolution of this fractal correlates well with the music of Frederic Chopin, Nocturne No. 19. Usually the video feedback is used

by artists for audio-to-video translation. The aim of such transformation is to gain a better perception of music [12]. The reverse transformation will also fulfil this task well.

6. DISLOCATIONS AND QUASI-ATTRACTOR

The image presented in Fig.8 is a typical video feedback pattern observed on the screen (compare with examples reproduced in Fig. 1.7 in [4]). Such a pattern is composed of regular light and dark strips which are parallel (never intersecting each other). However, dark strips are more visible on the bright background. Certain strips are broken up into smaller segments. The ends of segments form dislocations (see Fig. 9). This phenomena resemble a broken structure of convective rolls in fluid dynamics [9, 10], or even the dislocations in a crystal structure of metals or other single crystals, e.g. semiconductors, where the dislocation is the boundary of an extra atomic plane inserted into a perfect crystal structure [11]. Such defects can move, create or annihilate with temperature or strain. The same is in our pattern. With time, they also annihilate by coalescing of the two neighbouring strips (see, for example, the marked strips in Figs. 9a,b).
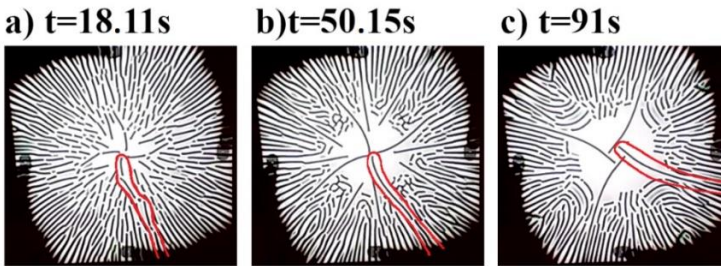
Fig. 9. Samples of the fractal from Fig.7 showing dislocations (marked by red line)

The patterns collected in Figures 8a,b,c, are similar, yet different in spatial detail. Therefore, the pattern composed from four-fold 'star' in the central part, and the laminar structure outside is a quasi-attractor according to the definition introduced by J.P. Crutchfield [1]. A quasi-attractor is associated with global space features. In this case it is a star which rotates in time, yet its shape is stable.

7. CONCLUSIONS

The category of video feedback dynamics depends mainly on the overall magnification M and on the angle α of the camera-monitor combination.

When the M is less than one, the 'a monitor inside a monitor' is displayed.

This kind of picture is stationary, fractal, with a clear scaling symmetry. The modification of the set-up to the aparatous consisting of two or three camera set-u results in generation of a popular fractals, such as Sierpinski gasket, for example. This category was presented in details in Paper I. In the present paper, two selected dynamic fractals were demonstrated. One from the category temporally repeating images, and second from spatially decorrelated dynamics. The second image clearly illustrates a new kind of attractor, the quasi-attractor. The intriguing shape of this pattern and its temporal behaviour correlates adequately with Chopin music.

REFERENCES

[1] James P. Crutchfield, Space-time dynamics in video feedback, Physica I'0D (1984) 229-245,

[2] Michael C. Andersen, Jesper Peterson, Simulation of videofeedback,(1996) (http://web.archive.org/web/20120829103456/http://www.videofeedback.dk/vf/ss/sspost.html)

[3] S.A. Collins, K.C. Wasmundt, Optical Feedback and bistability: a review, Opt. Eng.19 (1980) 478.

[4] H.O. Peitgen, H. Jurgens, D. Saupe, Chaos and Fractals, Springer Verlag, N.Y.1992.

[5] P. Bałuka, I. Mielniczek,V. Druz, J. Chabko, M. Kuzma, Optical Feedback. I Static Effects, Physics for Economy, vol.5/ 2023, pp. 71- 85.

[6] A.M. Turing, The Chemical Basis of Morphogenesis, Philosophical Transactions of the Royal Society of London. Series B, Biological Sciences, Vol. 237, No. 641. (1952), pp. 37-72.

[7] Courtial, J., Leach, J., & Padgett, M. J. (2001). Fractals in pixellated video feedback. Nature, 414(6866), 864-864.

[8] Ang K.H., Chong, G.C.Y., Li, Y. PID control system analysis, design, and technology. IEEE Transactions on Control Systems Technology 13(4), (2005) 559-576.

[9] J.A. Whitehead, The propagation of dislocations in Rayleigh-Benard rolls and bimodal flow, J. Fluid Mech. (1976), vol. 15, part 4, pp. 715-720.

[10] Abbas Alwi Sakhir Abed and Ahmed Abdel Kadhim Majhoo, Wave Convection Regimes in an Inclined Layer of Nano Fluid, Int.J. of Current Engineering and Technology Vol. 5, No. 1 (2015) 539-543.

[11] C. Kittel, Introduction to Solid State Physics, John Wiley and Sons, N.Y.2018.

[12] E.M. Kim, An Artistic Technique for Audio-to-Video Translation on Music Perception Study, Int.J. of Multimedia & Applicationsv.4 No3 (2012) 11-19.

[13] Video 1: https://pwswpl-my.sharepoint.com/:v:/g/personal/p_baluka_s_pansp_pl/EXC4IGzaKWxHqNsFhWX02fIBMJrbqsdrQKp34DPQLjcDLQ?nav=eyJyZWZlcnJhbEluZm8iOnsicmVmZXJyYWxBcHAiOiJPbmVEcml2ZUZvckJ1c2luZXNzIiwicmVmZXJyYWxBcHBQbGF0Zm9ybSI6IldlYiIsInJlZmVycmFsTW9kZSI6InZpZXciLCJyZWZlcnJhbFZpZXciOiJNeUZpbGVzTGlua0RpcmVjdCJ9fQ&e=BRilxc

[14] Video with music: https://pwswpl-my.sharepoint.com/:v:/g/personal/p_baluka_s_pansp_pl/ETjrXVC_uCxNmOuMDWoUoPwBTOdrLPMSdZuu5-VPMz9ETg?

nav=eyJyZWZlcnJhbEluZm8iOnsicmVmZXJyYWxBcHAiOiJTdHJlYW1XZWJBc
HAiLCJyZWZlcnJhbFZpZXciOiJTaGFyZURpYWxvZyIsInJlZmVycmFsQXBwUG
xhdGZvcm0iOiJXZWIiLCJyZWZlcnJhbE1vZGUiOiJ2aWV3In19&e=lIXpwf